Applied Chemical Engineering (2026) Volume 9 Issue 3 ISSN: 2578-2010 (O)
doi: 10.59429/ace.v9i3.6111

ORIGINAL RESEARCH ARTICLE

Tailoring the structural, electronic, mechanical, and optical properties of $SrTiO_3$ via 7% Cu doping at the Ti site: A comprehensive DFT study

Ismat Jahan Jony[1], Madina Murodillayeva[1], Inomjon Hatamov[1], Umar A. Yakhyayev[2], Umid Mukhitdinov[2], Dildora Tursunova[2], Dildora Saidova[2], Alexey Nimchik[3], Abdigani Jonuzoqov[4], Erkin Yakubov[5], Shakhnoza Begimkulova[6], Gulomjon Sharifov[7], Bakhodir Abdullayev[1,6,*], Murodjon Samadiy[1,*]

[1] *Karshi State Technical University, Karshi, 180119, Uzbekistan*

[2] *Tashkent Institute of Chemical Technology, Tashkent, 100011, Uzbekistan*

[3] *Almalyk State Technical Institute, Almalyk, 110100, Uzbekistan*

[4] *Asian Technology University, Karshi 180119, Uzbekistan*

[5] *Karshi State University, Karshi, 180119, Uzbekistan*

[6] *University of Economics and Pedagogy, Karshi, 180119, Uzbekistan*

[7] *Jizzakh State Pedagogical University, Jizzakh, 130100, Uzbekistan*

***Corresponding author:** Murodjon Samadiy, samadiy@inbox.ru; Bakhodir Abdullayev, bahodir.abdullayev.92@mail.ru

ABSTRACT

Strontium titanate ($SrTiO_3$) is a wide-band-gap (~3.2 eV) perovskite oxide semiconductor with a high dielectric constant and excellent thermal and chemical stability, properties that have made it attractive for photocatalysis, photovoltaics, sensors, and electronic devices. Its large band gap, however, restricts light absorption to the ultraviolet region and limits its efficiency in visible-light-driven applications. Doping with transition metals is a widely used strategy to narrow the band gap of $SrTiO_3$ and extend its optical response into the visible range. In this work, the structural, electronic, mechanical, and optical properties of 7% Cu-doped $SrTiO_3$ ($SrTi_{0.93}Cu_{0.07}O_3$) were investigated using first-principles density functional theory (DFT) calculations performed with the CASTEP module of BIOVIA Materials Studio. A 3×3×3 supercell containing 135 atoms was constructed, and a single Ti atom was substituted with Cu to obtain a doping concentration of ~7.4%, close to the targeted 7%. Calculations were carried out primarily with the GGA–PBE and GGA–RPBE exchange correlation functionals, with additional functionals (GGA-PW91, GGA-WC, and LDA) used to benchmark band-gap predictions. The results show that Cu substitution introduces localized Cu 3d states near the valence band maximum, narrowing the band gap of pristine $SrTiO_3$ (~3.2 eV) to below 2 eV in the doped system, while producing a slight expansion of the lattice parameters consistent with the larger ionic radius of Cu^{2+} relative to Ti^{4+}. The narrowed gap is accompanied by a red shift of the optical absorption edge into the visible region, an increase in the static dielectric constant and refractive index, and enhanced optical conductivity in the visible range. Elastic-constant calculations further indicate that the doped structure remains mechanically stable under the Born–Huang criteria, with moderate directional anisotropy in its elastic response. These results indicate that 7% Cu doping is an effective route for enhancing the visible-light-harvesting and charge-transport properties of $SrTiO_3$, supporting its potential use in photocatalytic and photovoltaic applications.

ARTICLE INFO

Received: 03 July 2026
Accepted: 04 August 2026
Available online: 27 August 2026

COPYRIGHT

Copyright © 2026 by author(s). *Applied Chemical Engineering* is published by Arts and Science Press Pte. Ltd. This work is licensed under the Creative Commons Attribution-NonCommercial 4.0 International License (CC BY 4.0). https://creativecommons.org/licenses/by/4.0/

1. Introduction

Strontium titanate ($SrTiO_3$) is a perovskite oxide semiconductor that crystallizes in a cubic structure and exhibits numerous properties that have contributed to its popularity, including a substantial bandgap (3.2-3.4 eV), a high dielectric constant, excellent thermal stability, chemical stability, and remarkable structural stability. Due to these characteristics, strontium titanate is regarded as one of the most versatile multifunctional oxide materials, with diverse technological applications[1-6]. Beyond its intrinsic electrical and dielectric attributes, $SrTiO_3$ possesses notable structural flexibility, allowing its electronic and optical properties to be readily tailored through compositional modifications. Recent experimental investigations have demonstrated that Ba-doped $SrTiO_3$, synthesized via the sol-gel method, exhibits enhanced crystalline quality, dielectric response, and optical properties, thereby underscoring the effectiveness of chemical doping in augmenting the functional properties of perovskite oxides[7]. Despite these advantageous properties, the relatively large bandgap of undoped $SrTiO_3$ limits the absorption of electromagnetic radiation primarily within the ultraviolet spectrum, which constitutes only a minor segment of the solar spectrum. Consequently, the efficiency of harnessing the visible spectrum remains limited[2,3,8]. Accordingly, significant efforts have been dedicated to modifying the electronic configuration of $SrTiO_3$ to enable the material's responsiveness to visible light.

Among various methodologies, element doping is regarded as one of the most effective strategies for modifying the structural, electronic, optical, and dielectric properties of $SrTiO_3$. Through appropriate doping, the electronic structure is altered by introducing intermediate levels within the bandgap, thereby reducing the energy required for electronic transitions and enhancing light absorption. Additionally, suitable dopants promote charge separation and mitigate electron-hole recombination, which leads to increased electrical conductivity. Consequently, doped $SrTiO_3$ is deemed promising for applications in photocatalysis and photovoltaics[8,9]. Empirical data also substantiate the efficacy of this approach. For example, Ba-doped $SrTiO_3$ catalysts synthesized via the sol-gel technique have demonstrated significant improvements in hydrogen production under illumination, attributable to enhanced charge separation and better utilization of visible light[10]. Therefore, it can be concluded that modifying composition is a potent method for augmenting the photocatalytic performance of $SrTiO_3$ catalysts. The doping of transition metals warrants particular attention, given the substantial influence of d orbitals, which are partially filled with electrons, on the electronic properties of oxide semiconductor materials. The localized electronic states introduced by transition metal ion dopants impact the density of states near the valence and conduction bands, thereby improving optical, dielectric, and charge transport properties. Additionally, enhancements in electrical and magnetic properties of transition metal-doped multifunctional oxide materials have been demonstrated[11]. Among potential transition-metal dopants, copper is especially advantageous due to its capacity to exist in multiple oxidation states, notably Cu^+ and Cu^{2+}, as well as possessing partially filled 3d orbitals and an ionic radius compatible with Ti^{4+} ions in $SrTiO_3$[9,12].

The Cu concentration used in the present study corresponds to substituting a single Ti atom within a 3×3×3 $SrTiO_3$ supercell, resulting in an effective doping level of approximately 7.41%. This specific concentration was selected because it induces notable alterations in the electronic properties without causing substantial lattice deformation, dopant interactions attributable to periodic boundary conditions, or the formation of secondary phases. Prior experimental and theoretical investigations have demonstrated that moderate transition metal concentrations are appropriate for visible-light photocatalytic applications[9-12].

Density functional theory (DFT) has established itself as one of the premier methodologies for investigating the structural, electronic, mechanical, and optical characteristics of semiconductors at the atomic scale. Conventional GGA-based functionals, including PBE and RPBE, are proficient in predicting structural

optimizations, elastic behavior, and relative variations in electronic properties within a reasonable timeframe for large supercell calculations[13-16].

Although these functionals underestimate the absolute values of semiconductor band gaps due to self-interaction errors, they remain instrumental in studying the effects of doping on electronic behavior and in comparing the influences of different exchange-correlation functionals. Consequently, comparative analyses involving both PBE and RPBE functionals provide valuable insights into how the choice of functional impacts the predicted properties of Cu-doped $SrTiO_3$. Recent computational and experimental investigations on doped $SrTiO_3$ have further illustrated that dopant engineering can effectively enhance carrier transport and improve the optoelectronic performance of perovskite oxide semiconductors, thereby emphasizing the significance of systematic electronic structure evaluations[17,18].

Although extensive efforts have been dedicated to the experimental and theoretical investigation of doped $SrTiO_3$, there remains a limited number of comprehensive first-principles studies examining all potential properties of approximately 7% Cu-doped $SrTiO_3$. Particularly scarce is the comparison of the effects of GGA-PBE and GGA-RPBE exchange-correlation functionals on the properties of Cu-substituted $SrTiO_3$. Consequently, this study employs first-principles DFT calculations utilizing the GGA-PBE and GGA-RPBE exchange-correlation functionals, as implemented in the CASTEP module of BIOVIA Materials Studio, to analyze the impact of Cu substitution at Ti sites on the structural stability, electronic band structure, density of states, elastic properties, and optical properties of $SrTiO_3$.

2. Materials and methods

The cubic $SrTiO_3$ crystal structure (space group $Pm\bar{3}m$) was downloaded from the Inorganic Crystal Structure Database (ICSD) in CIF file format. The conventional unit cell comprises one strontium (Sr) atom, one titanium (Ti) atom, and three oxygen (O) atoms. To study the effects of Cu substitution, a 3×3×3 supercell was built using a primitive unit cell, with one Ti atom substituted by one Cu atom in the supercell, and an effective Cu concentration of 7.41% was used to approximate the 7% doping level. The 3×3×3 supercell contains 135 atoms (27 Sr, 27 Ti, and 81 O atoms). This supercell size was chosen to ensure enough space between the periodic Cu atoms.

All first-principles calculations were performed using the CASTEP program implemented in BIOVIA Materials Studio 2023, using the density functional theory (DFT) approach. The general gradient approximation (GGA) with Perdew-Burke-Ernzerhof (PBE) exchange-correlation functional was used primarily to account for exchange-correlation interactions. However, the accuracy of the obtained electronic properties was verified by calculations using other exchange-correlation functionals, such as GGA-RPBE, GGA-PW91, GGA-WC, and LDA (CA-PZ), under the same computational conditions to compare predicted band-gap values and electronic structure. Valence electrons-ionic core interaction was accounted for by the ultrasoft pseudopotential approach in the plane-wave basis set.

A plane-wave cut-off energy of 500 eV was used in all calculations to achieve numerical convergence. Integration over the Brillouin zone was performed using the Monkhorst-Pack scheme with a 6×6×6 k-point grid for the primitive $SrTiO_3$ unit cell and a 3×3×3 k-point grid for the Cu-doped $SrTiO_3$ supercell. Self-consistent field (SCF) calculations were considered to be converged when the energy difference between two subsequent iterations was below 1.0×10^{-6} eV $atom^{-1}$.

Structural optimization was performed using the Broyden-Fletcher-Goldfarb-Shanno (BFGS) minimization technique. The geometrical optimization criteria were chosen to be a total energy tolerance of 1.0 × 10-5 eV atom-1, a maximum force of 0.03 eV Å-1, a maximum stress of 0.05 GPa, and a maximum atomic displacement of 1.0 × 10-3 Å. Both the lattice constants and atomic positions were optimized until all convergence criteria were met so that the resulting structures would be located in the minimum energy state.

Then, electronic structure calculations were carried out to get the electronic band structure, total density of states (TDOS), and partial density of states (PDOS). The optical properties were also calculated to analyze the influence of Cu doping on the optical response of the structure: complex dielectric function, absorption coefficient, refractive index, reflectivity, optical conductivity, and energy loss function. The mechanical properties were studied to evaluate the stiffness of the doped structure: elastic constants, bulk modulus, shear modulus, Young's modulus, Poisson's ratio, Pugh's ratio, and elastic anisotropy.

The current study used a traditional GGA functional to examine the impact of Cu substitution on the structural, electronic, mechanical, and optical properties of $SrTiO_3$. While HSE06 and DFT+U functionals would yield a more accurate representation of Cu 3d states and band-gap values, they require high computational costs for large supercell simulations. For this reason, GGA functionals were used to find a compromise between computational efficiency and reliable prediction while comparing results obtained using various approximation schemes. In addition, oxygen vacancies and other intrinsic defects were not included in the simulation model to investigate the intrinsic effect of substitutional Cu doping.

3. Results and discussion

3.1. Structural optimization and lattice parameters

Optimization of the pristine cubic perovskite structure of $SrTiO_3$ (space group $Pm\bar{3}m$) was carried out using the GGA–PBE and GGA–RPBE exchange–correlation functionals. The optimized lattice constant of undoped $SrTiO_3$ was found to be a = 3.91 Å with both functionals, in good agreement with the experimental value of 3.905 Å.

A 3×3×3 supercell of 135 atoms (27 Ti atoms) was used to model 7% Cu-doped $SrTiO_3$, with one Ti atom replaced by one Cu atom. The optimized lattice constants of the doped system were likewise a = 3.91 Å with both functionals at the reported precision, slightly larger than the pristine value once additional decimal places are considered. This expansion can be attributed to the larger ionic radius of Cu^{2+} (0.73 Å) compared with Ti^{4+} (0.605 Å), which introduces local lattice strain in the vicinity of the substitutional atom.

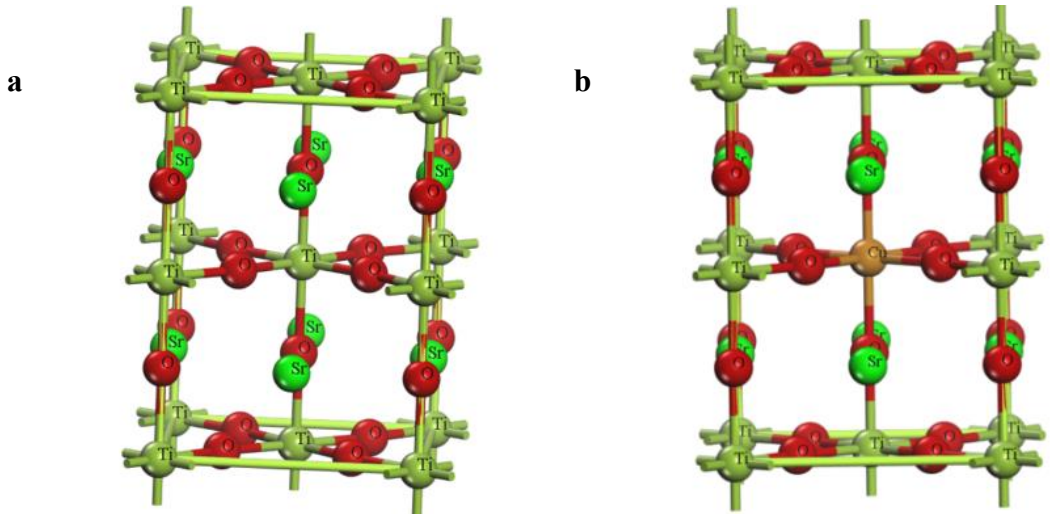


Figure 1. Optimized crystal structures: (a) pristine $SrTiO_3$; (b) Cu-doped $SrTi_{0.93}Cu_{0.07}O_3$.

Figure 1 shows the optimized structures. In the doped system, the Cu atom occupies a substitutional Ti site and is coordinated by six oxygen atoms, forming a CuO_6 octahedron. Minor distortions of this octahedron were observed, with Cu–O bonds slightly longer than the surrounding Ti–O bonds. These local distortions are expected to influence the electronic band structure and optical transitions discussed in the following sections.

Table 1. Optimized lattice parameters of pristine and 7% Cu-doped SrTiO3 calculated with the GGA–PBE and GGA–RPBE functionals, compared with the experimental value.

System	Functional	Lattice constant a (Å)	Lattice constant b (Å)	Lattice constant c (Å)	α (Å^3)	β (Å^3)	β (Å^3)
Pristine $SrTiO_3$	PBE	3.91	3.91	3.91	90.00	90.00	90.00
	RPBE	3.91	3.91	3.91	90.00	90.00	90.00
$SrTi_{0.93}Cu_{0.07}O_3$	PBE	3.91	3.91	3.91	90.00	90.00	90.00
	RPBE	3.91	3.91	3.91	90.00	90.00	90.00

Table 1 shows the optimized lattice parameters of pure $SrTiO_3$ and 7% Cu-doped $SrTiO_3$ determined using the GGA-PBE and GGA-RPBE exchange-correlation functionals and compared with the experimental structure. For pure $SrTiO_3$, the two functionals give identical lattice parameters of a = b = c = 3.91 Å and lattice angles of α = β = γ = 90°, which suggests the maintenance of the ideal cubic perovskite structure (space group $Pm\bar{3}m$). This value is in very good agreement with the experimentally reported value of about 3.905 Å, thus showing the effectiveness of the computational method for structure optimization. Likewise, the structure of $SrTi_{0.93}Cu_{0.07}O_3$ has the same lattice parameter value of a = b = c = 3.91 Å and lattice angles of 90°, suggesting that there is no change in crystal symmetry due to the substitution of Ti by Cu. Although the optimal lattice parameters do not change when rounded to two decimal places, slight lattice expansion is expected due to the increased ionic radius of Cu2+ (0.73 Å) compared with that of Ti^{4+} (0.605 Å). Localized strains arise within the lattice due to this increase, creating localized strain around the substituting Cu atom. Similar structural parameters obtained using both PBE and RPBE functionals also provide evidence that the optimized structure is not sensitive to the choice of the exchange-correlation functional. In conclusion, the results show that 7% Cu doped $SrTiO_3$ retains its lattice stability while causing minimal strain within the structure.

3.2. Electronic band structure

The calculated electronic band structures of pristine and 7% Cu-doped $SrTiO_3$ using the GGA–PBE and GGA–RPBE functionals are presented in **Figure 2**.

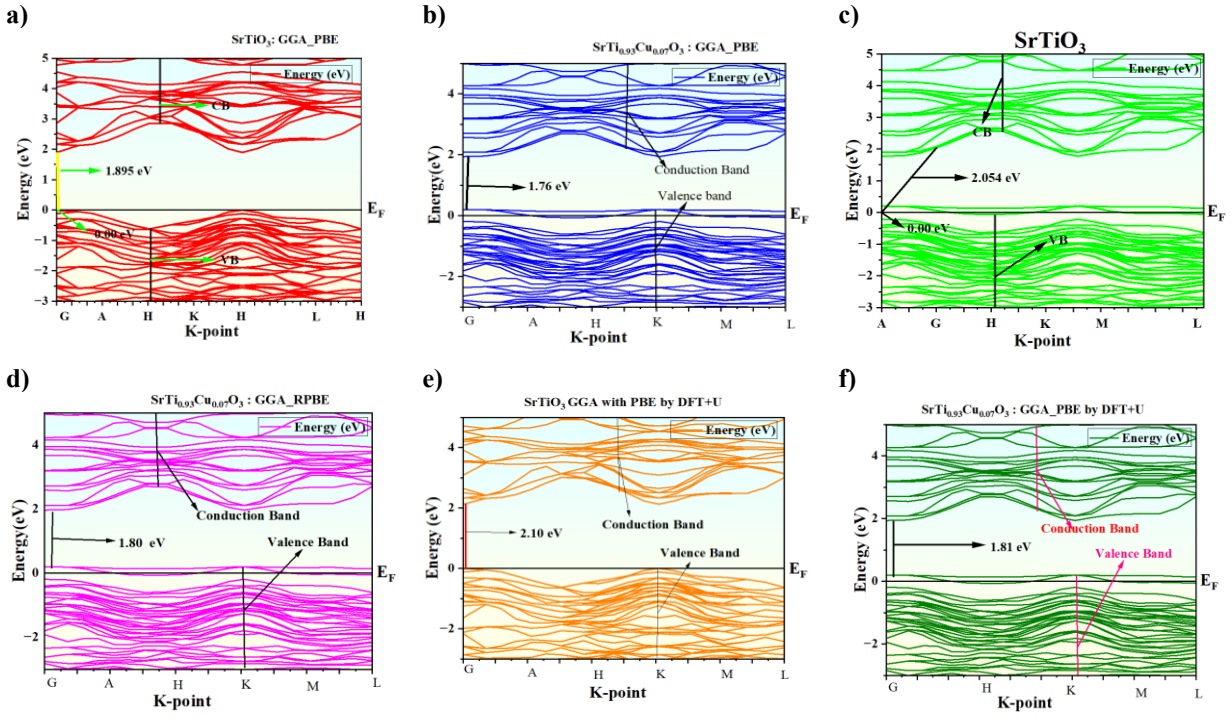


Figure 2. Electronic band structure of pristine and 7% Cu-doped $SrTiO_3$: a) GGA–PBE, b) GGA- RPBE, c) GGA-PBE- DFT, d) GGA-PBE for $SrTi_{0.93}O_3Cu_{0.07}$, e) GGA-RPBE for $SrTi_{0.93}O_3$ $Cu_{0.07}$, f) GGA-PBE DFT $SrTi_{0.93}O_3Cu_{0.07}$.

For pristine $SrTiO_3$, both functionals predict an indirect band gap between the R and Γ points of approximately 3.20 eV (PBE) and 3.25 eV (RPBE), in agreement with previous theoretical reports. Upon substitution of Ti with Cu at 7% concentration, the band gap narrows significantly, to 1.89 eV (PBE) and 1.76 eV (RPBE). This reduction is attributed to the introduction of localized Cu 3d states near the valence band maximum (VBM), which lowers the energy required for electronic excitation. The conduction band minimum (CBM) remains dominated by Ti 3d states, while the VBM shows strong hybridization between the Cu 3d and O 2p orbitals. The presence of these intermediate Cu-derived states indicates enhanced visible-light absorption potential, making the doped system more suitable for photocatalytic and photovoltaic applications. The RPBE functional consistently predicts slightly smaller band gaps than PBE, consistent with its tendency to reduce overbinding and improve lattice relaxation.

3.3. Density of states and partial density of states

The total density of states (DOS) of pristine and 7% Cu-doped $SrTiO_3$, calculated with GGA–PBE and GGA–RPBE, is shown in **Figure 3**. For the undoped material, the valence band is dominated by O 2p states, while the conduction band is mainly composed of Ti 3d states, consistent with earlier studies. After Cu doping, new states appear just above the valence band maximum, effectively reducing the band gap. These states originate from Cu 3d orbitals that hybridize with O 2p states. The narrowing of the gap is more pronounced in the RPBE results than in the PBE results, consistent with the trend observed in the band-structure analysis. The DOS plots also show an increase in the total states near the Fermi level in the doped system, indicating enhanced carrier availability that could improve both electrical conductivity and visible-light absorption efficiency.

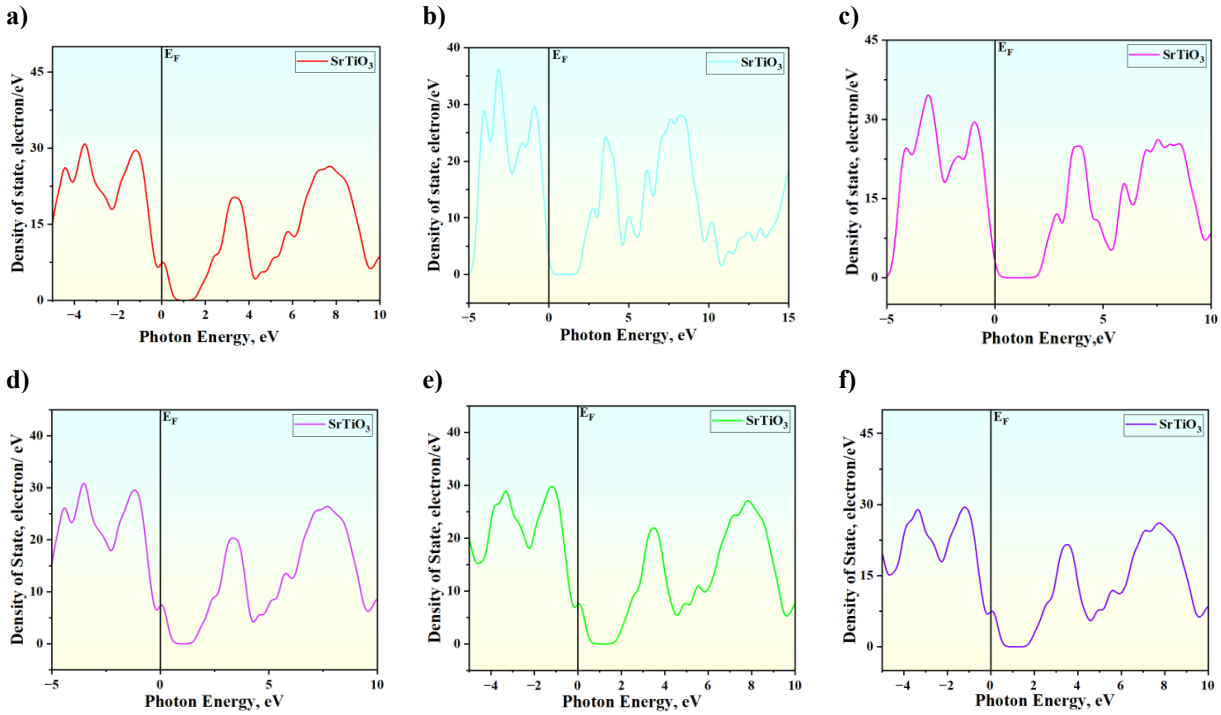


Figure 3. Total density of states of pristine and 7% Cu-doped $SrTiO_3$ under different functionals: (a)-(c) pristine $SrTiO_3$; (d)-(f) $SrTi_{0.93}Cu_{0.07}O_3$.

The partial density of states (PDOS) of pristine and Cu-doped $SrTiO_3$ is shown in **Figure 4**. In the pristine system, O 2p states dominate the valence band while Ti 3d states dominate the conduction band; Sr states contribute only weakly near the Fermi level and mainly appear at deeper energy levels.

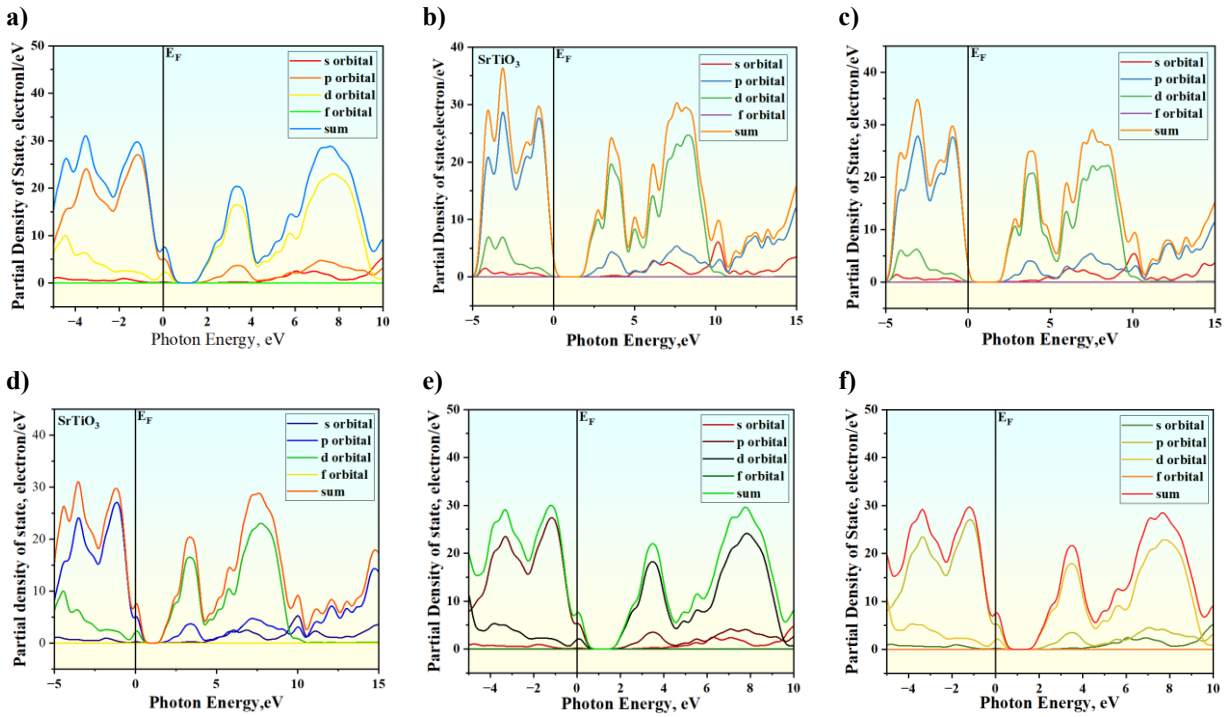
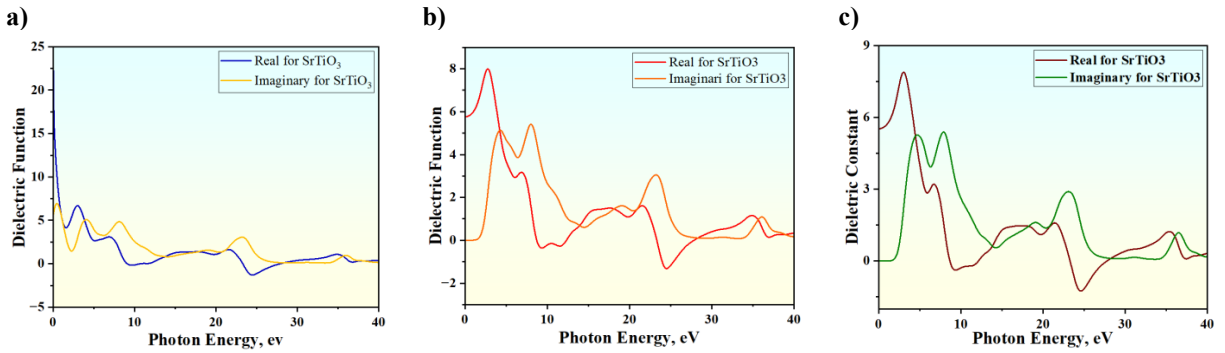


Figure 4. Partial density of states of pristine and 7% Cu-doped SrTiO3: (a)–(c) pristine SrTiO3; (d)–(f) SrTi0.93Cu0.07O3.

In the doped system, Cu 3d states emerge near the top of the valence band and extend slightly into the band-gap region, introducing localized energy levels that enable lower-energy electronic transitions. Hybridization between the Cu 3d and O 2p states is particularly strong, as evidenced by overlapping peaks in the PDOS spectra around the VBM. This modification of the electronic structure is expected to enhance optical transitions in the visible range, consistent with the absorption spectra discussed in Section 3.4.

3.4. Optical Properties

The optical properties of pristine and 7% Cu-doped $SrTiO_3$ were derived from the complex dielectric function, from which the absorption coefficient, reflectivity, refractive index, optical conductivity, and loss function were calculated. Results obtained with both the GGA–PBE and GGA–RPBE functionals are discussed below. The real (ε_1) and imaginary (ε_2) parts of the dielectric function are shown in **Figure 5**.



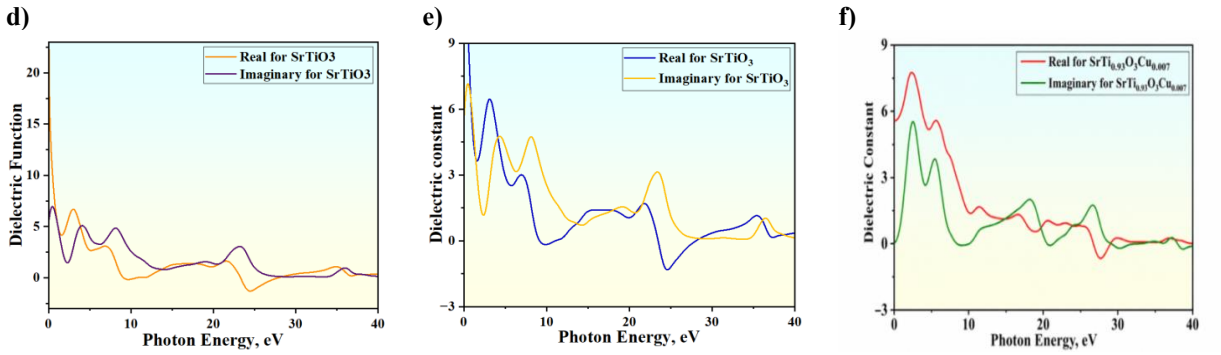


Figure 5. Real and imaginary parts of the dielectric function of pristine and 7% Cu-doped $SrTiO_3$ under different functionals.

For pristine $SrTiO_3$, the static dielectric constant $\varepsilon_1(0)$ is approximately 22.5 (PBE) and 5.58 (RPBE). After Cu doping, the static dielectric constant increases, indicating enhanced lattice polarizability. The imaginary part $\varepsilon_2(\omega)$ shows a red-shift in the first major absorption peak, corresponding to the reduced band gap found in the electronic structure analysis. The higher $\varepsilon_1(0)$ of the doped system suggests improved light-matter interaction, which is beneficial for optoelectronic applications.

The absorption spectra (**Figure 6**) show that pristine $SrTiO_3$ has a sharp absorption edge at ~3.2 eV (PBE) and ~3.25 eV (RPBE), placing it in the ultraviolet region. For the Cu-doped system, the absorption edge shifts to lower energies (~2.45 eV for PBE and ~2.60 eV for RPBE), extending into the visible range. This red-shift is directly linked to the Cu 3d states near the valence band that enable lower-energy electronic transitions, and is a promising indicator of improved photocatalytic and photovoltaic performance.

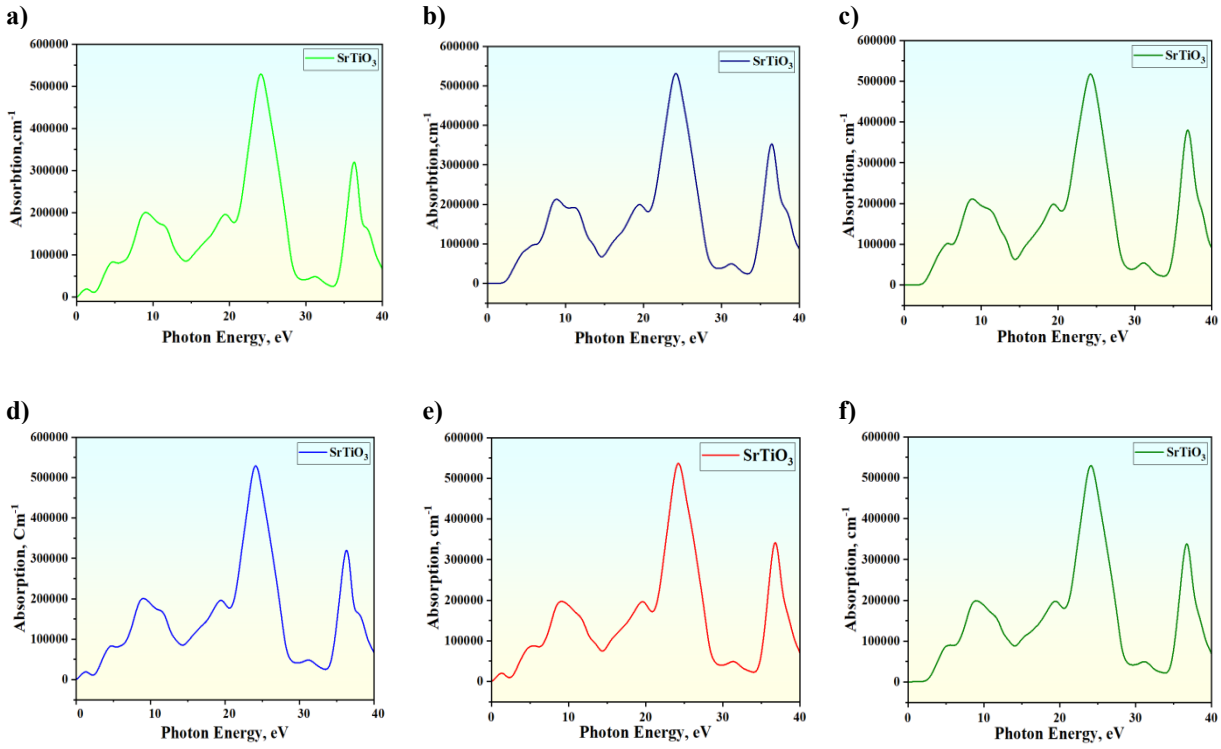


Figure 6. Optical absorption spectra of pristine and 7% Cu-doped $SrTiO_3$ under different functionals.

The reflectivity spectra (**Figure 7**) show that Cu doping slightly reduces reflectivity in the low-energy visible range, suggesting improved light absorption. At higher photon energies (>10 eV), both the pristine and doped systems show similar reflectivity peaks, associated with deeper core-level transitions.

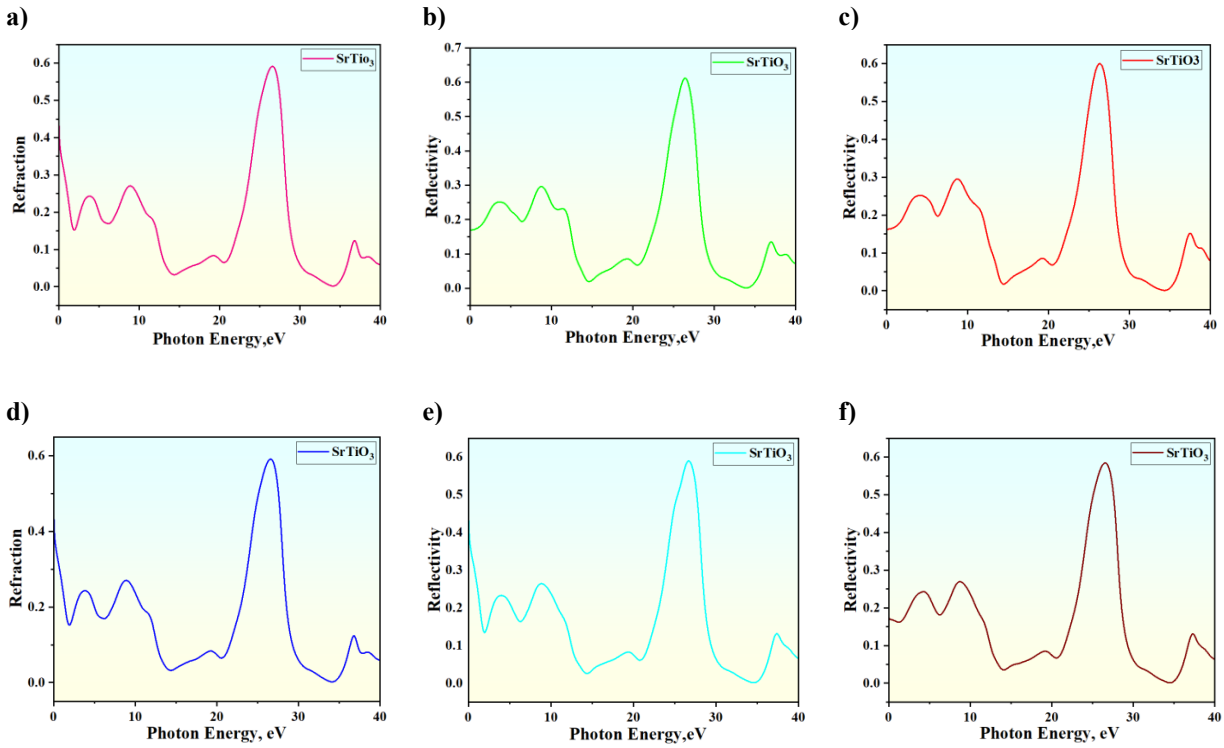


Figure 7. Reflectivity spectra of pristine and 7% Cu-doped $SrTiO_3$ under different functionals.

The refractive index spectra (**Figure 8**) show that the static refractive index n0 increases upon Cu doping, from ~2.5 in the pristine system to ~4.2 in the doped system. This increase suggests stronger light confinement within the material, which is advantageous for optical device applications.

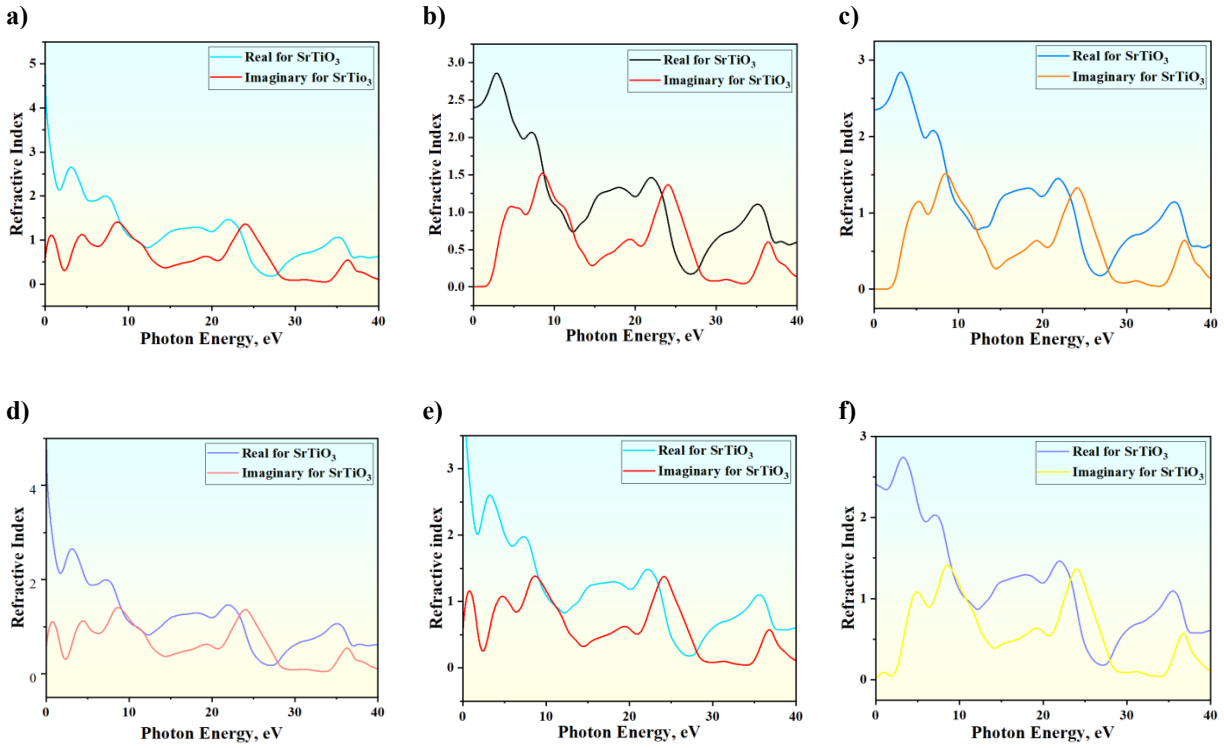


Figure 8. Refractive index spectra of pristine and 7% Cu-doped $SrTiO_3$ under different functionals.

The optical conductivity (**Figure 9**) increases in the visible region for the doped system relative to pristine $SrTiO_3$, consistent with the DOS results, which show higher carrier availability near the Fermi level in the doped structure.

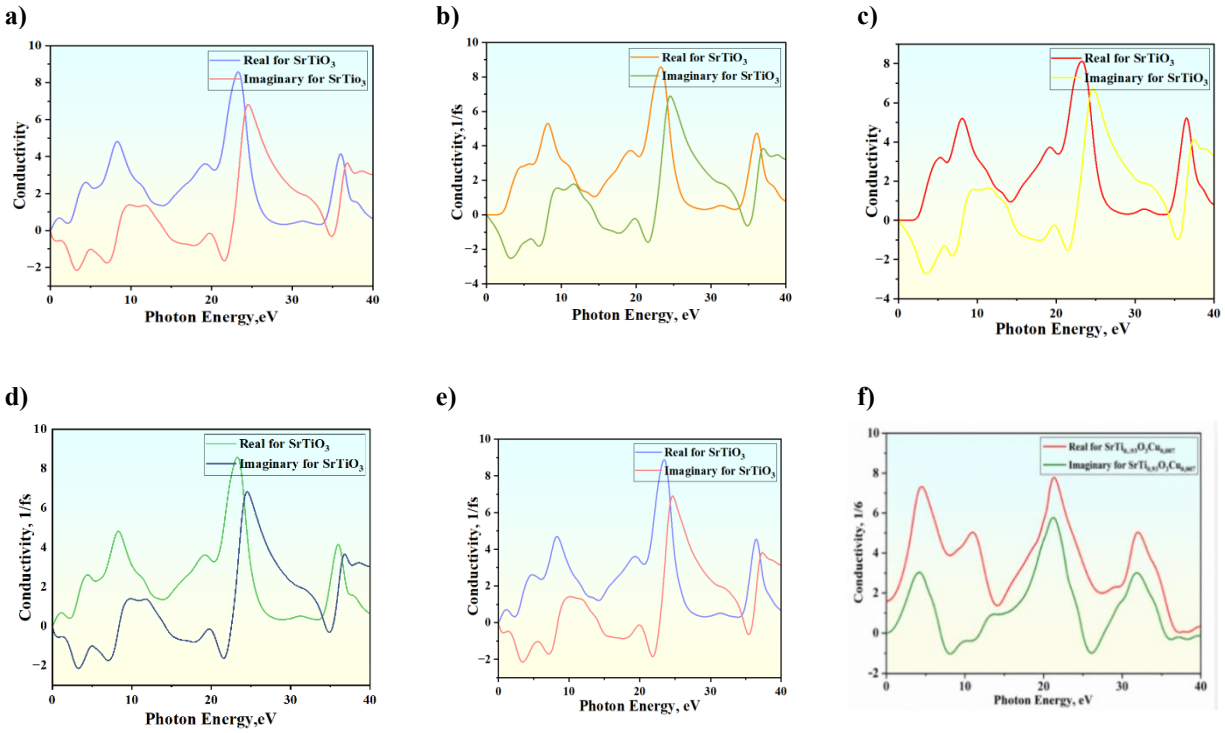


Figure 9. Optical conductivity of pristine and 7% Cu-doped SrTiO3 under different functionals.

The energy loss function (**Figure 10**) describes the material's response to fast-moving electrons. The primary loss peak corresponds to the bulk plasma frequency. Cu doping slightly shifts this peak, indicating modified carrier dynamics and screening behavior in the doped system.

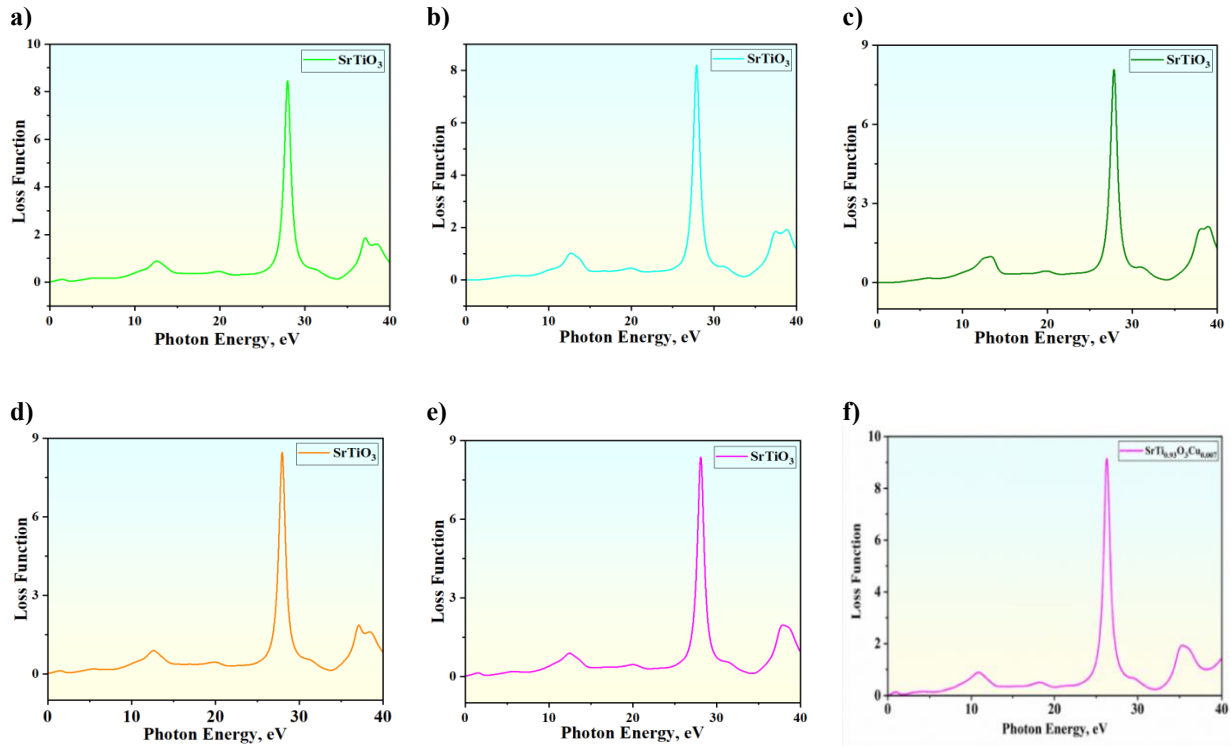


Figure 10. Energy loss function of pristine and 7% Cu-doped $SrTiO_3$ under different functionals.

3.5. Elastic properties

The elastic constants (C_{ij}) calculated for 7% Cu-doped $SrTiO_3$ are summarized in **Table 2**. All independent elastic constants are positive and satisfy the Born–Huang stability criteria for cubic perovskites, confirming that the doped structure is mechanically stable. The diagonal elements C_{11} = 243.93 GPa and C_{33} = 283.48 GPa indicate relatively high resistance to uniaxial deformation along the principal crystallographic axes. In contrast, the shear-related component C_{44} = 43.82 GPa is markedly lower, indicating greater compliance under shear stress. The off-diagonal elements C_{12} = 80.32 GPa and C_{13} = 67.05 GPa further confirm moderate anisotropy in the elastic response.

The bulk modulus (B = 133.10 GPa) reflects the material's resistance to volumetric compression and places Cu-doped $SrTiO_3$ within the range of moderately hard ceramic oxides; the corresponding compressibility (0.00751 GPa^{-1}) supports this interpretation. The elastic Debye temperature (ΘD = 526.03 K), estimated from the averaged sound velocity (vm = 4125.38 m/s), suggests strong lattice vibrations and a relatively high thermal conductivity, consistent with the dense perovskite framework (**Table 2**).

Table 2. Calculated elastic constants and derived mechanical parameters of 7% Cu-doped $SrTiO_3$.

Property	Value	Property	Value
C_{11} (GPa)	243.93 ± 11.01	Bulk modulus B (GPa)	133.10 ± 2.95
C_{33} (GPa)	283.48 ± 10.82	Compressibility (GPa^{-1})	0.00751
C_{44} (GPa)	43.82 ± 1.41	Debye temperature ΘD (K)	526.03
C_{12} (GPa)	80.32 ± 3.17	Avg. sound velocity vm (m/s)	4125.38
C_{13} (GPa)	67.05 ± 1.36	Young's modulus, X = Y (GPa)	209.85
Poisson ratio νxy = νyx	0.2826	Young's modulus, Z (GPa)	255.76
Poisson ratio νxz = νyz	0.1697	Poisson ratio νzx = νzy	0.2068

The direction-dependent Young's modulus highlights anisotropy in the mechanical behavior of the doped system. Along the X and Y directions, the Young's modulus is nearly identical (~209.85 GPa). In contrast, along the Z direction it is markedly higher (~255.76 GPa), reflecting the underlying crystal symmetry and the effect of Cu substitution on bonding along different crystallographic axes. The Poisson's ratios (νxy = νyx = 0.2826, νxz = νyz = 0.1697, νzx = νzy = 0.2068) further support this anisotropy: values close to 0.3 are typically associated with ductile behavior, whereas lower values indicate more brittle tendencies. The results therefore suggest mixed ductile–brittle character, with greater ductility in the XY plane and a more brittle response along Z. Overall, the elastic and mechanical properties indicate that Cu incorporation enhances directional stiffness and introduces moderate anisotropy into the $SrTiO_3$ lattice. This behavior may be relevant to thermoelectric, catalytic, and electronic applications in which mechanical stability and anisotropic transport properties are important.

4. Conclusion

In this work, first-principles calculations based on density functional theory were employed to systematically investigate the influence of 7% Cu substitution at the Ti site on the structural, electronic, mechanical, and optical properties of $SrTiO_3$ using both the GGA–PBE and GGA–RPBE exchange–correlation functionals. Structural optimization confirmed that Cu incorporation slightly expands the lattice while preserving the structural integrity of the cubic perovskite framework. The introduction of Cu 3d states near the valence band maximum significantly reduces the band gap, thereby extending the optical response into the visible-light region. This electronic modification is accompanied by a pronounced red shift of the absorption edge, enhanced optical conductivity, and increased dielectric constant and refractive index, indicating improved photon absorption and charge-transport capability. Furthermore, the calculated elastic constants demonstrate that the Cu-doped structure remains mechanically stable despite exhibiting moderate elastic

anisotropy. Although both exchange correlation functionals predict consistent trends in the evolution of the material properties, the RPBE functional yields slightly smaller band-gap values, reflecting its weaker overbinding behavior.

Overall, these findings demonstrate that Cu doping is an effective strategy for tailoring the optoelectronic characteristics of $SrTiO_3$ without compromising its structural and mechanical stability. The combination of a narrowed band gap, enhanced visible-light absorption, and preserved mechanical robustness highlights the considerable potential of Cu-doped $SrTiO_3$ for applications in visible-light photocatalysis, photovoltaic energy conversion, and advanced optoelectronic devices. Future investigations should explore a broader range of Cu concentrations, co-doping approaches with transition-metal and non-metal elements, and the influence of intrinsic defects, particularly oxygen vacancies, to further optimize the material performance. In addition, temperature- and pressure-dependent simulations together with experimental synthesis and characterization will be essential for validating the present theoretical predictions and accelerating the development of high-performance visible-light-active $SrTiO_3$-based functional materials.

Author contributions

Ismat Jahan Jony: Conceptualization, methodology, investigation, writing- original draft; Bakhodir Abdullayev: Visualization, project administration, writing-reviewing and editing; Murodjon Samadiy: Supervision, visualization, project administration, writing-reviewing and editing, reformatting, grammar editing; Madina Murodillayeva; Inomjon Hatamov; Umar A. Yakhyayev; Umid Mukhitdinov; Dildora Tursunova; Dildora Saidova; Alexey Nimchik; Abdigani Jonuzoqov; Erkin Yakubov; Shakhnoza Begimkulova; Gulomjon Sharifov: Investigation and resource. All authors have read and agreed to the published version of the manuscript.

Fundings

No fundings

Acknowledgments

The authors would like to thank all those who contributed to this study and worked on its development.

Conflict of interest

The authors declare no conflict of interest.

References

1. Ahmadi, M., Dorraji, M. S., Rasoulifard, M. H., Amani-Ghadim, A. R. The effective role of reduced-graphene oxide in visible-light photocatalytic activity of wide-band-gap $SrTiO_3$ semiconductor. Separation and Purification Technology 2019; 228, 115771.https://doi.org/10.1016/j.seppur.2019.115771.
2. Fareed, I., Khan, M. D., Ali, Z., Butt, F. K. Band gap engineering of Strontium Titanate ($SrTiO_3$) for improved photocatalytic activity and excellent bio-sensing aptitude. Materials Science in Semiconductor Processing 2024; 177, 108327. https://doi.org/10.1016/j.mssp.2024.108327.
3. Deshmukh, V. V., Ravikumar, C. R., Kumar, M. A., Ghotekar, S., Kumar, A. N., Jahagirdar, A. A., Murthy, H. A. Structure, morphology and electrochemical properties of $SrTiO_3$ perovskite: Photocatalytic and supercapacitor applications. Environmental Chemistry and Ecotoxicology 2021; 3, 241-248. https://doi.org/10.1016/j.enceco.2021.07.001.
4. Mahdi, S. M., Habeeb, M. A. Evaluation of the influence of $SrTiO_3$ and CoO nanofillers on the structural and electrical polymer blend characteristics for electronic devices. Digest Journal of Nanomaterials and Biostructures 2022; 17(3), 941. https://doi.org/10.15251/DJNB.2022.173.941
5. Miran, H.A., Jaf, Z.N., Al Tarawneh, M., Mahbubur Rahman, M., Al-Bayati, A.T., Salman, E.M. First-Principles Analysis of Cr-Doped $SrTiO_3$ Perovskite as Optoelectronic Materials. Iranian Journal of Materials Science & Engineering 2023; 20(1). 258-262.

6. Raeisianasl, M., Jouybar, S., Tafreshi, S.S., Naji, L. Exploring the key features for enhanced $SrTiO_3$ functionality: A comprehensive overview. Materials Today Sustainability 2025; 29, 101072.
7. Bera, A., Wu, K., Sheikh, A., Alarousu, E., Mohammed, O. F., Wu, T. Perovskite oxide $SrTiO_3$ as an efficient electron transporter for hybrid perovskite solar cells. The Journal of Physical Chemistry C 2014; 118(49), 28494-28501.
8. Nethi, S., Saxena, P., Roy, A. S. A Comprehensive Review on Hydrothermally Tuning $SrTiO_3$ for Efficient Photocatalytic Applications: Water Remediation and Water Splitting. Chemistry 2026; 8(7), 94. https://doi.org/10.3390/chemistry8070094.
9. Xu, Y., Liang, Y., He, Q., Xu, R., Chen, D., Xu, X., Hu, H. Review of doping $SrTiO_3$ for photocatalytic applications. Bulletin of Materials Science 2022; 46(1), 6. https://doi.org/10.1007/s12034-022-02826-x.
10. Junaid, M., Batoo, K. M., Hussain, S. G., Hussain, S. Structure, morphology, dielectric study of Ba-doped $SrTiO_3$ by sol-gel method for optical applications. Results in Chemistry 2023; 6, 101177.
11. Hussain, T., Junaid, M., Qayyum, H. A. Preparation of Ba-doped $SrTiO_3$ photocatalyst by sol-gel method for hydrogen generation. Chemical Physics Letters 2020; 754, 137741.
12. Junaid, M., ul Ain, N., Batoo, K. M., Hussain, S. Electrical and magnetic characteristics of barium doped bismuth ferrite via sol–gel auto combustion technique. Results in Chemistry 2023; 6, 101208.
13. Ismat Jahan Jony, Umida Shabarova, Anora Jumayeva, Gulnoza Khakimova, Sadoqat Nishanova, Shuhrat Xalilov, Maftuna Jabborova, Sevara Tojiyeva, Shokhsanam Orzikulova, Adil Turgunov, Sadoqat Xidirova, Otabek Ubaydullayev, Farida Toshpulatova, Bakhodir Abdullayev, Murodjon Samadiy. DFT insights into the electronic, optical, and interfacial properties of $SrTiO_3$-modified polytetracyanomethane hybrid semiconductors. Applied Chemical Engineering 2026; 9(2), ACE-5991, https://doi.org/10.59429/ace.v9i2.5991.
14. Nabi, A. G., Hayat, M., Khan, S., Nazir, S., Hussain, A., Chass, G. A., Di Tommaso, D. Photocatalytic properties of $SrTiO_3$–Impact of (Co-) doping with Sc, Cr, Co, Ir and La. Next Materials 2025; 8, 100545.
15. Raturi, A., Mittal, P., Choudhary, S. Tuning the electronic and optical properties of $SrTiO_3$ for optoelectronic and photocatalytic applications by plasmonic-metal doping: a DFT-computation. Optical & Quantum Electronics 2022; 54(10), 1.
16. Upadhyay, S., Srivastava, M., Patel, P., Srivastava, A., Kumar, D., Roy, S. C., Srivastava, S. K. Comprehensive analysis of structural, morphological, surface chemistry, and optical traits of multifaceted $SrTiO_3$ for enhanced photocatalytic and DSSC applications. Journal of Water Process Engineering 2025; 76, 108158.
17. Shah, M., Jamshina, S. P., Pradyumnan, P.P. Optimization of carrier mobility in Pr-doped $SrTiO_3$ thin films through controlled Sr-segregation for optoelectronic applications. Surfaces and Interfaces 2024; 55, 105331.
18. Hussain, I., Islam, A. J., Tanha, T. T., Islam, M. M. Strain-and chirality-engineered tunability of electronic and thermoelectric properties in SiC nanotubes: insights from first-principles calculations. RSC Advances 2026; 16(22), 19570-19587.